*Journal of Structural Geology*, Vol. 8, No. 5, pp. 563 to 573, 1986
Printed in Great Britain

0191-8141/86 $03.00 + 0.00
Pergamon Journals Ltd.

# Two-dimensional refold interference patterns

RICHARD THIESSEN

Geology Department, Washington State University, Pullman, WA 99164, U.S.A.

(*Received* 27 *February* 1984; *accepted in revised form* 18 *March* 1985)

**Abstract**—When a rock undergoes two generations of folding, complex three-dimensional refolded structures result. If such a structure is then sectioned, two-dimensional interference patterns result. These patterns have been discussed before, but the incredible variety and complexities of these patterns can be shown only with a large number of diagrams. Using a computer simulation, various refolded structures have been sliced at every unique 30° combination of strike and dip (thirty sections per structure). The characteristics of the patterns observed are discussed and recurring recognizable patterns are identified.

## INTRODUCTION

WHEN a rock has undergone two stages of folding, a three-dimensional refold structure will result. These structures have been analyzed in the field and hand sample, but most ideas on refolding are generated using some type of model. Early workers (O'Driscoll 1962, Brown 1967) used card deck models to simulate refolds. Cards were cut into the first fold waveform and then were slid past one another in order to create the second folds. The first folds can be of any shape and nature (cylindrical, non-cylindrical, concentric, similar) but most modellers used similar cylindrical folds. The second folds, by the nature of the model, will also be similar cylindrical folds. The cards themselves are the shear planes of the second deformation, and will be parallel to the second fold axial planes (Carey 1962). In this type of modelling, bedding is assumed to be passive during the second folding episode. This modelling technique has the advantage of creating an easy-to-visualize three-dimensional model of the refold. However, each single model takes several hours to create.

Modelling of refolds using Plasticine (or other modelling clays) has been done by numerous workers (e.g. Holmes & Reynolds 1954, Watkinson 1981). The great advantage of Plasticine models is that layers of contrasting competency can be incorporated in the model. Anisotropic elements, such as boudins, lineations, or earlier fold hinges can also be included (Watkinson 1981). Plasticine models simulate behavior of geologic materials more realistically, but are again time consuming to create. They also require specialized laboratory equipment.

I have developed a computer program, REFOLD, which generates refold structures. The program was written as a general research tool and allows for the construction of multiple generations of folds of any orientation, waveform and amplitude, as well as pure shear, simple shear and faulting. Bedding thicknesses can be adjusted and the original bedding orientation can be varied. The resulting three-dimensional refold can then be 'cut' in any orientation to simulate map or outcrop patterns. The program has the same limitations as the card deck model: folds are assumed to be similar (shear) cylindrical folds with passive bedding. However, the great advantage of the computer model is that each refold takes mere seconds to generate. The program also designates the locations of the fold axial planes, which in some refolds are not that obvious.

Ramsay (1967, pp. 520–533) recognized four classes of three-dimensional refolds. These classes are distinguished by whether the first fold axes and/or the first fold axial planes are deformed during the second generation of folding. He used two angles, $\alpha$ and $\beta$, in his classification scheme. $\alpha$ is the angle between the original first fold direction ($f_1$) and the second kinematic fold axis ($b_2$). $\beta$ is the angle between the pole to the first axial plane ($c_1$) and the second slip direction ($a_2$). Thiessen & Means (1980) demonstrated that the angle $\alpha$ is not a good choice as a classification angle. They introduced two new angles, $\gamma$ and $\delta$. $\gamma$ is the angle from the first fold hinge direction ($f_1$) to the pole to the second axial plane ($c_2$). $\delta$ is the angle between the poles to the two axial planes ($c_1$ and $c_2$), which also equals the angle between the axial planes themselves.

Angles $\beta$ and $\gamma$ are definitive angles for refold classification. Thiessen & Means (1980) showed that when $\beta = 90°$,the first axial plane is not folded by the second folds. When $\gamma = 90°$, the first fold hinges are not folded by the later folds. These two angles can then be used to distinguish the types of refolds Ramsay (1967) discussed. Type 0 refolds (trivial or sinusoidal) are ones in which neither the first fold hinges or axial planes are folded. These are trivial cases that would not appear to be refolds. They instead would resemble a single episode of folding, and so are not discussed further here. Type 1 refolds (basin and dome) are structures in which the first fold hinges are folded but the axial planes are not ($\beta = 90°$, $\gamma \neq 90°$.

Type 2 refolds (crescent) are typified by both the first hinges and axial planes being folded ($\beta \neq 90°$, $\gamma \neq 90°$), while type 3 refolds (coaxial or hook) have straight first hinges and folded first axial planes ($\beta \neq 90°$, $\gamma = 90°$).

Thiessen & Means (1980), as a part of their study,

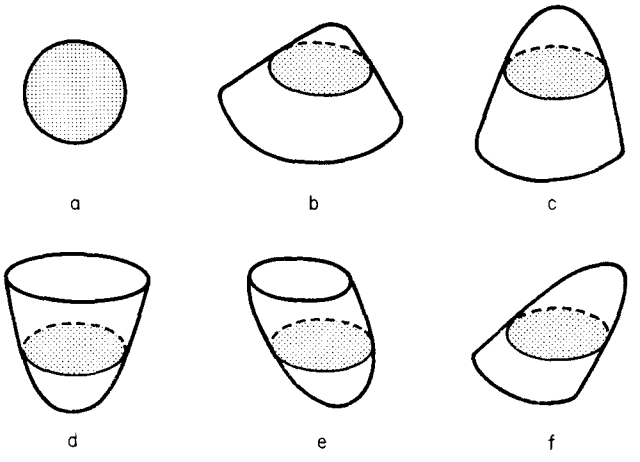


Fig. 1. A circular two-dimensional refold pattern (a), that might be seen on a map, and various three-dimensional refold structures that could create this map pattern. (b) and (c) show vertical domes, (d) shows a vertical basin, and (e) and (f) show an oblique basin and dome, respectively.

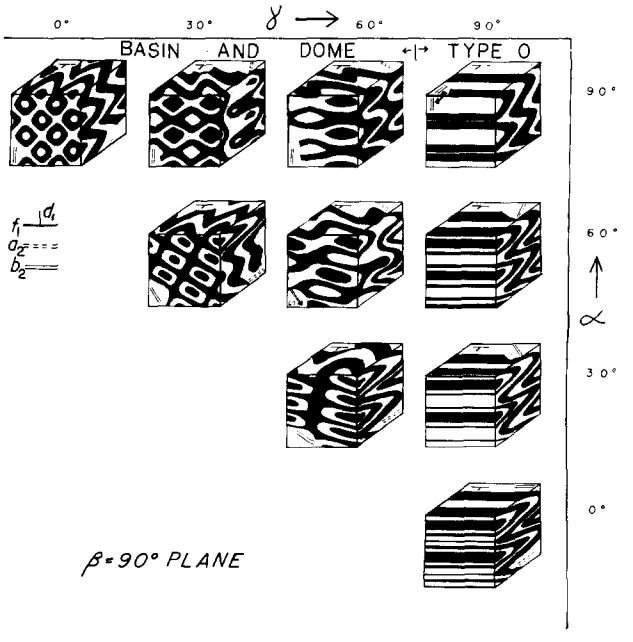


Fig. 2. Refold examples from the plane of all ideal basin and dome and type 0 (sinusoidal) refold cases ($\beta = 90°$). The first fold form can be seen in the upper right hand cube. $a_2$ and $b_2$ orientations are shown with dashed and solid double lines. Bedding was initially parallel to the front faces of the cubes.

prepared a series of two-dimensional interference patterns through one type 2 crescent refold. Their exercise showed that a wide variety of patterns can be generated by cutting differently oriented sections through one three-dimensional refold structure. That is, a refold structure is not characterized by only one possible two-dimensional pattern. The reverse is also true. A single two-dimensional interference pattern can be created by an infinite number of refold geometries. Figure 1(a) shows a circular refold pattern, as might be seen on a map or section. This pattern is typical of a basin and dome (type 1) refold. Without further data, one could not tell if the structure were a vertical dome (Figs. 1b & c), a vertical basin (Fig. 1d), an oblique basin (Fig. 1e), or an oblique dome (Fig. 1f). The solution to this problem could, of course, be constrained by structural data such as fold hinge plunges or strikes and dips of whatever surface is defining the refold (bedding, foliation). The relative ages of units at the center of the structure vs those on the outside margin should tell if the structure is basinal or domal, as long as one has way-up indicators. Three-dimensional data, such as a vertical outcrop in the map area or sequential levels in a mine, will also constrain the geometry of the refold structure.

This problem becomes even more complex when one considers the wide variety of possible fold shapes and asymmetries that could interfere to create a refold. Interpretation of a refold pattern might appear to be an almost insurmountable task. However, to aid in this interpretation, a series of refold patterns have been generated using the REFOLD program. They are reproduced here to illustrate the wide variety of possible refold patterns. These patterns are all generated with symmetric first folds, and both folding episodes as sine waves of equal amplitude and wavelength. The orientations of the two phases of folding are related by the angles $\alpha$, $\beta$, $\gamma$ and $\delta$, as well as the orientation volume that Thiessen & Means (1980) defined and used.

*Type 1 patterns*

Type 1 interference is probably the most familiar type of refold pattern. Familiar names for it are 'basin and dome' and 'egg-carton' shapes. This type of pattern appears on the back face of the orientation volume, where $\beta = 90°$. Representative cases on the back face of the orientation volume are shown in Fig. 2. A series of cubes for different values of $\alpha$ and $\gamma$ are depicted. Bedding was originally parallel to the front face of the cubes. The first folds were sinusoidal with horizontal axial planes and horizontal axes ($f_1$) parallel to the top edge of the front face. The uppermost right corner cube, which is an example of a type 0 trivial refold, shows the first fold waveforms. The second folding episode had a different orientation for each of the cubes, but they all were of the same form and amplitude as the first folds. For each cube, $b_2$ is shown with a short double solid line, while $a_2$ is shown with a short double dashed line. These are all located on one of the surfaces of each cube, except for the $\alpha = \gamma = 60°$ case, where $b_2$ plunges at an angle of 60 degrees into the front face of the cube.

The upper left cube of Fig. 2 shows the classic 'egg-carton' pattern of 'basins and domes'. When $\alpha$ is close to 90°, the 'basins and domes' align along the two fold axes. But when $\alpha$ is not a right angle, the patterns are arranged en échelon to the fold axes, as noted by O'Driscoll (1962). When the two folding episodes are symmetric, the bedding plane, which is parallel to the front faces of the cubes, will be thrown into symmetric shapes for the top edge ($\alpha = 90°$) of Fig. 2. The axial planes are the symmetry planes. The diagonal bottom edge ($\alpha + \gamma = 90°$) also shows symmetric patterns, but the symmetry planes are at an angle to the fold orientations. The

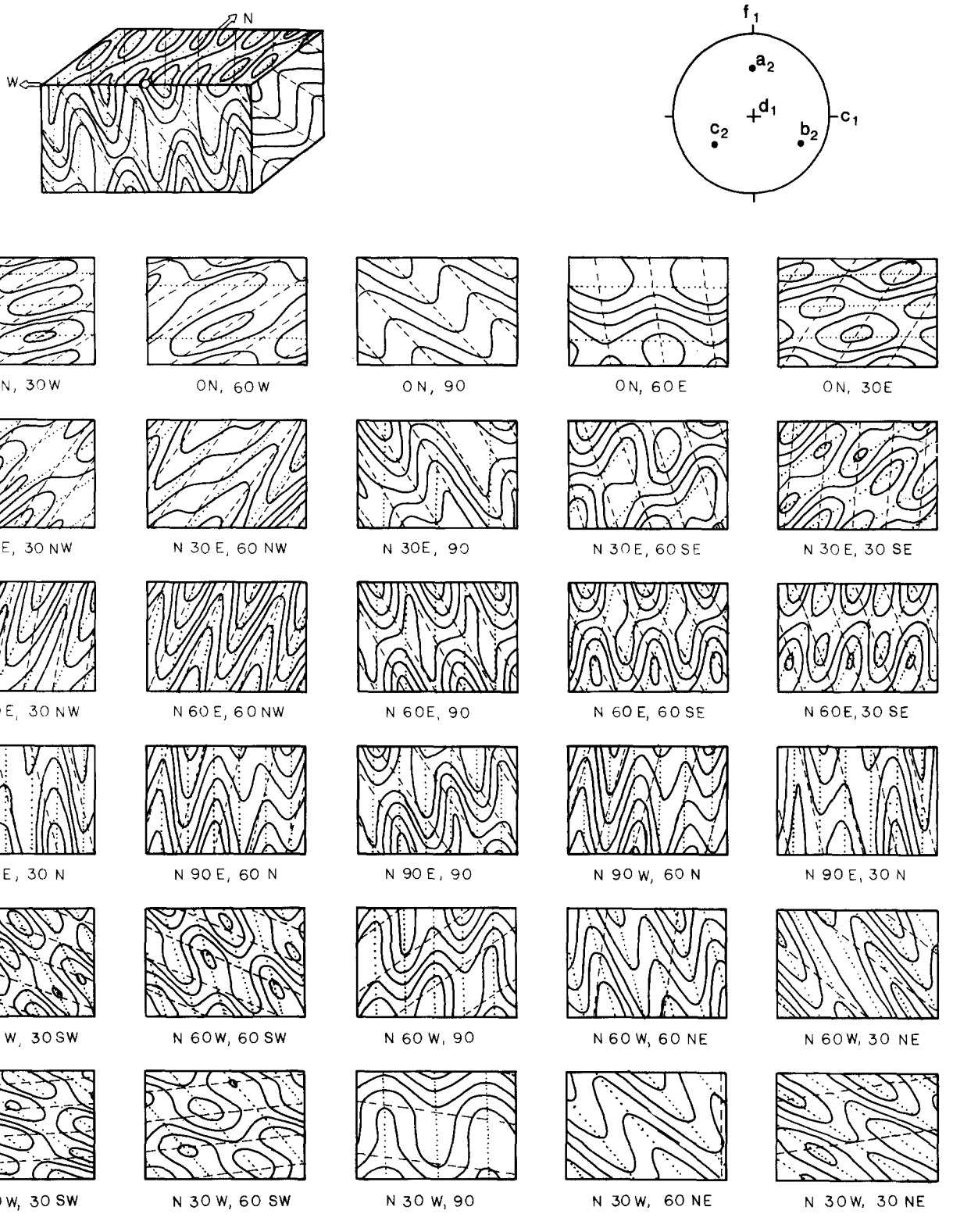


Fig. 3. A basin and dome refold, showing the wide variety of two-dimensional refold patterns that are possible. Values of the parameters that define the interference are $\alpha = 60°$, $\beta = 90°$, $\gamma = 60°$, $\delta = 45°$. The three-dimensional block in the upper left is oriented with N to the back and W to the left. Bedding was originally horizontal. Kinematic axes are shown in the stereonet, upper right. Sections are shown for every 30° combination of strike and dip. Dotted and dashed lines show the traces of the first and second fold axial planes, respectively.

bottom edge also will have one bed forming a continuous network around all the 'basins and domes'.

The right-hand column of Fig. 2 is the region of type 0 patterns. Notice that these vary from 'refolds' in which one sees only the first fold waveforms to 'refolds' in which the two fold generations directly add to create simple sinusoidal waveforms.

Figures 3 and 4 show the variety of two-dimensional patterns that can be obtained from 'basin and dome' interference. The first case has the values of $\alpha = \gamma = 60°$, $\beta = 90°$ and $\delta = 45°$. The latter case is the ideal 'basin and dome' example, where $\alpha = \beta = \delta = 90°$ and $\gamma = 0°$. At the top of both of these figures is shown a block with N oriented towards the back of the block, and E to the

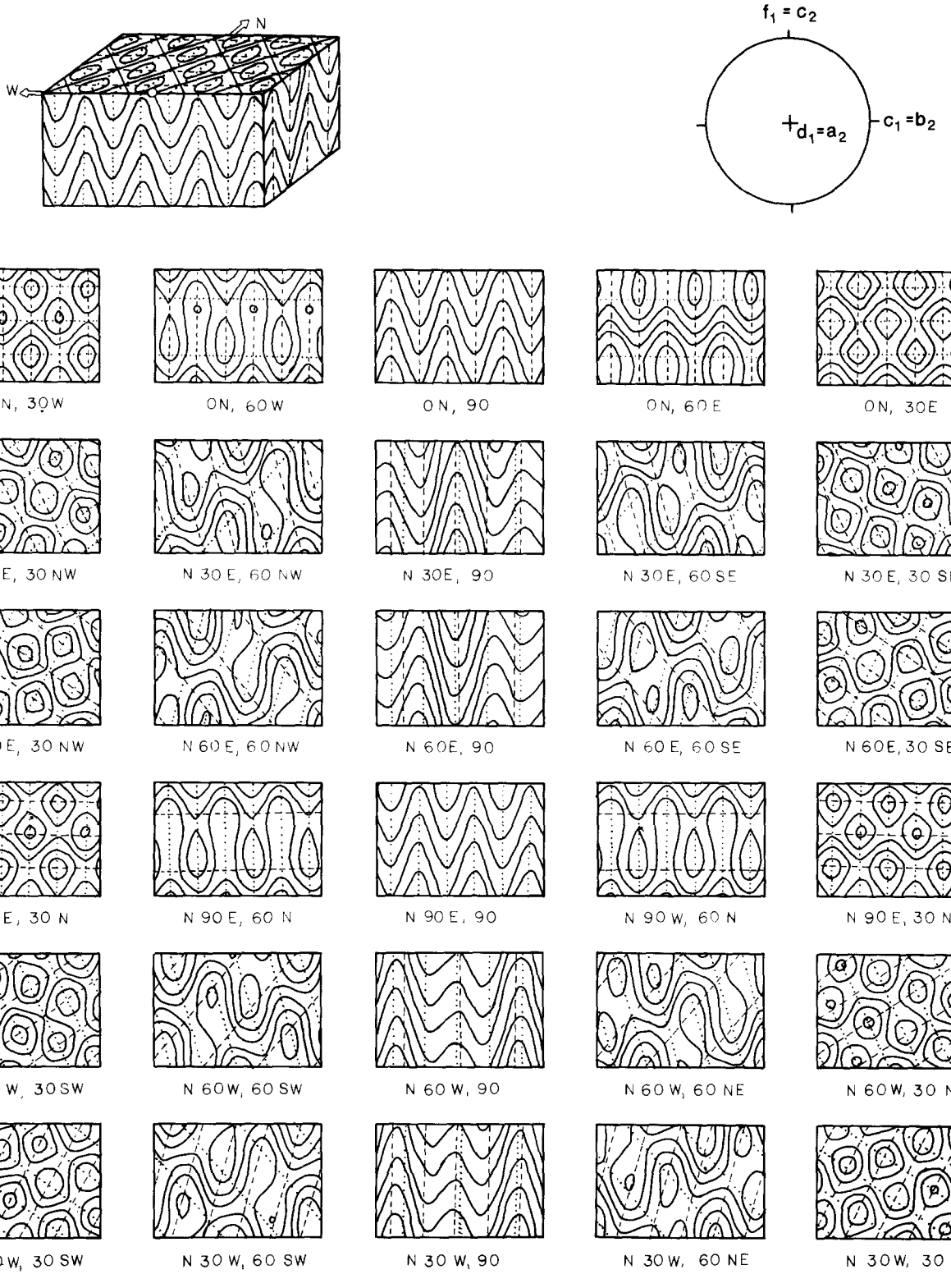


Fig. 4. The ideal basin and dome refold, with the first and second axial planes at right angles to each other ($\alpha = 90°$, $\beta = 90°$, $\gamma = 0°$, $\delta = 90°$). Conventions are the same as in Fig. 3. This refold occurs at the back left corner of Thiessen & Means' (1980) orientation volume. Note the variety of refold patterns that are possible.

right. A reference origin is placed at the midpoint of the top front edge of the block. First folds were oriented N–S, with vertical axial planes, while bedding was originally horizontal. For the second folds of Fig. 3, $b_2$ trends S 54°E and plunges 30°, while the axial plane strikes N 35°W and dips 60°E. In Fig. 4, the axis of second folding motion is E–W with a vertical axial plane. The lower part of each of the diagrams shows two-dimensional interference patterns obtained on various sections cut through the block. Strikes, measured clockwise from N, and dips are given for each plane. The lower patterns are depicted for all unique 30° combinations of strike and dip. These sections show that type 1 two-dimensional patterns include sinusoidal waves, basins and domes, circles, and tear-drop shapes.

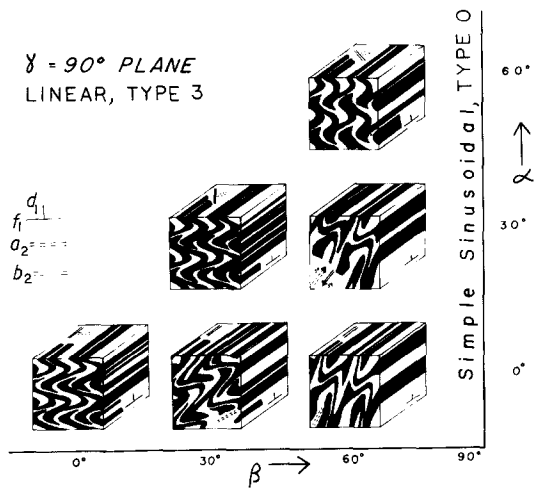


Fig. 5. The plane of ideal type 3 (linear) refolds, where $\gamma = 90°$. The first axial planes were initially parallel to the right hand cube faces. The first folds had horizontal fold axes. Second fold orientations are as shown. Note the linear patterns that occur on the top and side cube faces. The type 0 (sinusoidal) field occupies the right hand edge of this diagram, which is equivalent to the right hand edge of Fig. 2.

*Type 3 patterns*

This type of interference pattern occurs along the right-hand side of the orientation volume. Figure 5 shows some of the variations in type 3 refolds. For all of the cubes shown in Fig. 5, the first folds were oriented N–S with vertical axial planes and horizontal fold axes. Bedding was originally parallel to the top faces of the cubes. For this type, $\gamma = 90°$, therefore the first fold axes are not bent by the second folding motions. So, the first fold hinge lines show up as straight lines in the three-dimensional pattern, as do all linear elements of the first folds parallel to the hinge lines. The two-dimensional patterns that appear on the front faces of the cubes of Fig. 5 will be repeated linearly along the $f_1$ direction in the third dimension. There are therefore a whole family of planes, containing $f_1$, which will show the startling refold interference pattern of straight lines. A glance at Fig. 5 will show that on one of these planes, the beds will not necessarily occur in stratigraphic order and in fact can appear several times in the sequence on one cross-section or outcrop.

The front faces of the cubes show varieties of patterns that feature hooks. Ramsay called this pattern the diagnostic type 3 refold pattern, but Thiessen & Means (1980) demonstrated that hook patterns can occur in type 2 refolds. Examples of these will be shown later in this report. These hooks are best formed along the $\alpha = \gamma$ diagonal. It was stated previously that all viewing sections containing $f_1$ will show straight lines. All other cross-sections will show spread-out versions of the front faces of the cubes in Fig. 5. No other two-dimensional patterns are possible. If one sees any closed patterns, such as circles, triangles, crescents, or rectangles, then the refold cannot be type 3.

*Type 2 patterns*

In most geologic examples of refolding, both the first fold axes and axial planes are deformed by the second folding episode. All these cases will plot in the type 2 field. A wide variety of two-dimensional patterns are possible in this type, as indicated in Figs. 6–9. These figures have the same conventions as Figs. 3 and 4. Figure 6 shows an example of a refold classified by Thiessen & Means (1980) as a triangular refold. Ramsay would have called this a $(1 \rightarrow 2)$ refold. It is in the transition zone between 'basin and dome' refolds and crescent refolds. Figure 7 shows the crescent refold that is at the upper left front corner of the orientation volume, which is the furthest point from both the 'basin and dome' and coaxial refold fields. Figures 8 and 9 show crescent refolds that have the same values of $\alpha$, $\beta$ and $\gamma$, but different values of $\delta$. These refolds come from the center of the orientation volume, where two possible refold geometries exist for each point. Points on the outer faces of the orientation volume represent one distinct refold geometry, and so only one value of $\delta$ exists for each of these points.

Figures 7–9 show many interesting patterns. Each shows variations of hook patterns, which were originally thought to occur only in type 3 refolds. Other patterns include arrows, crescents, bird's heads, sine waves, W's and M's, S's and Z's, and rather unpredictable patterns. A rather intriguing pattern can be seen on the top face of the block in the upper left corner of Fig. 7. This surface appears to contain simple sine waves. However, closer examination will reveal that the sine waves are generated by only two beds which are repeated across the top of the block. This repeated sine wave pattern can occur on sections cut parallel to the original bedding orientation. If the first folds were originally symmetric, then repeated sine wave patterns can occur in all type 2 refolds that plot along the front curved face of the orientation volume. If the first folds are not constrained to be symmetric, then any type 2 refold could exhibit repeated sine wave patterns.

*Observed ranges of interference patterns*

Figure 10 shows a sampling of distinctive refold patterns that might occur on a section through a three-dimensional refold. These include sine wave (S), repeated sine wave (RS), crescent (C), hook (H), arrow (A), S or Z shape (Z), W or M shape (W), dog's tooth (D), triangular (T), perpendicular (P), bird's head (B), basin and dome (BD), and straight line (L). Most of these shapes are self explanatory. The dog's tooth pattern is a variation on the hook pattern in which the hooks themselves do not extend to the next fold hinge and so do not have bent tips. The bird's head pattern is a hook with the core of the hook tip being occupied by another bed. The perpendicular pattern is an interesting one in which folds of sine wave shape interact to form box-shaped folds. An example can be seen in Fig. 6 where the cross section strikes N 60°E and dips 60°NW.

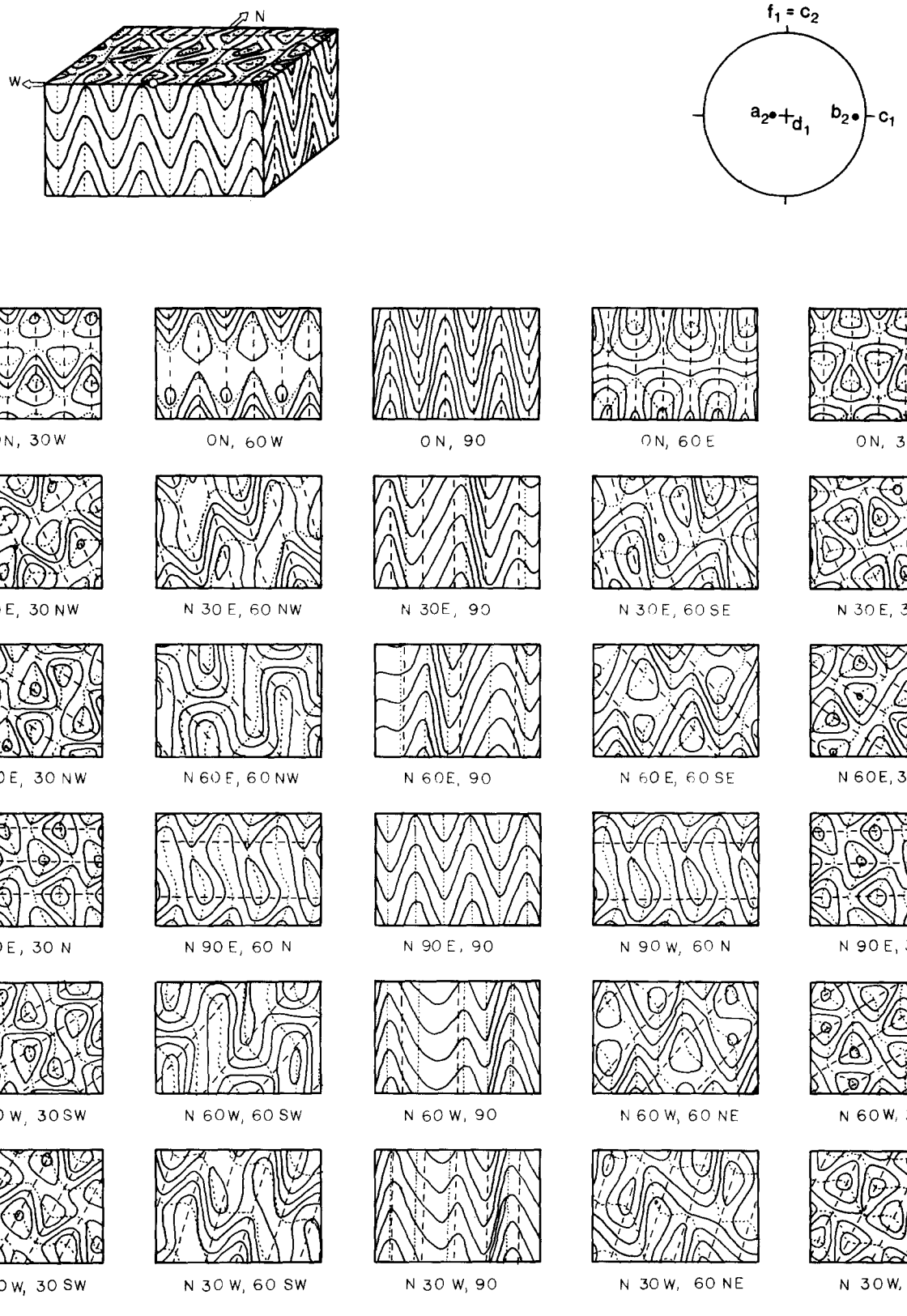


Fig. 6. A triangular (type 1 → 2) refold, showing a variety of possible refold patterns. Conventions are as in Fig. 3.

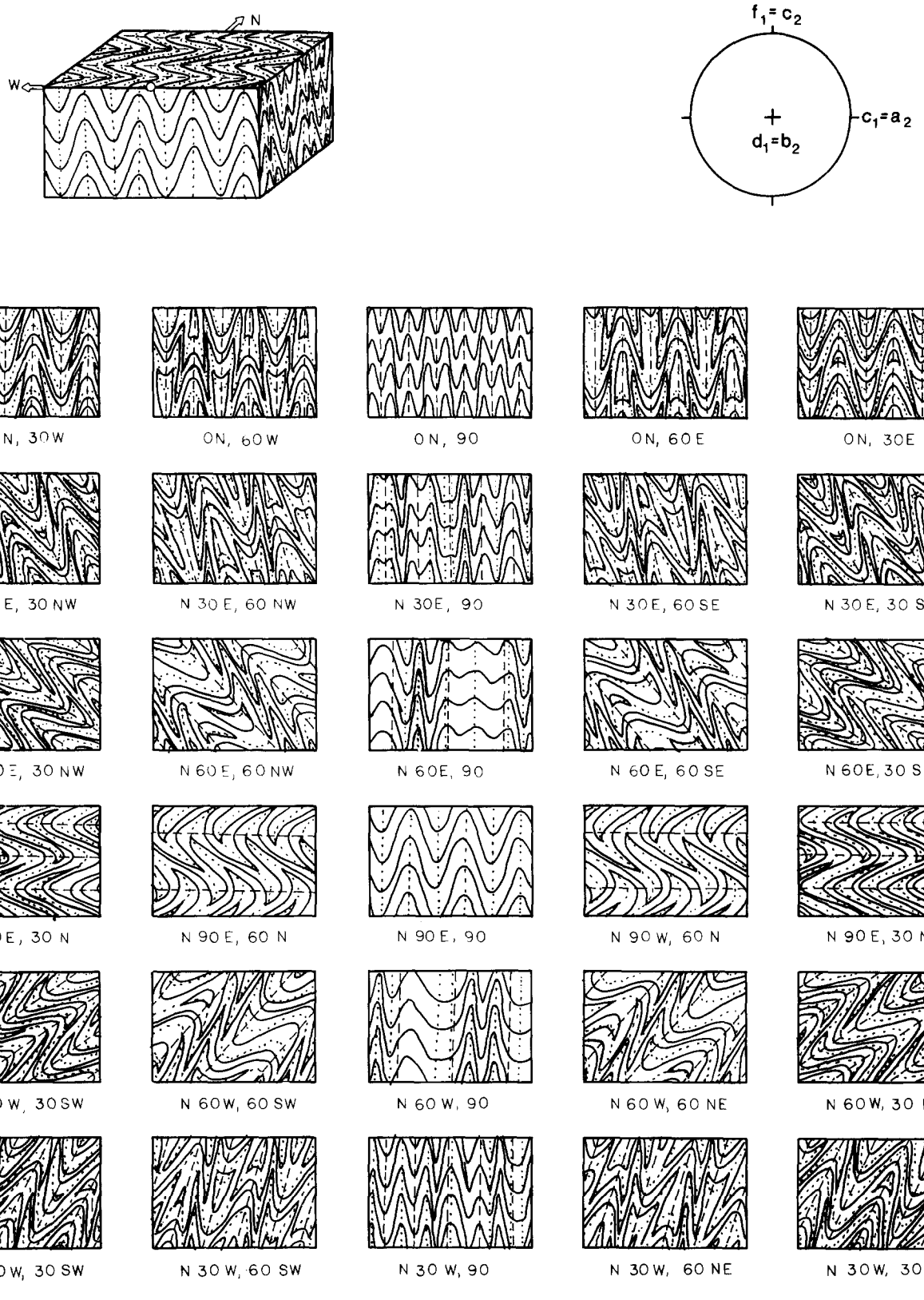


Fig. 7. The type 2 (crescent) refold structure that occurs at the front upper left corner of the orientation volume, and the two-dimensional patterns that can be observed. Conventions are as in Fig. 3, and with $\alpha = 90°$, $\beta = 0°$, $\gamma = 0°$, $\delta = 90°$.

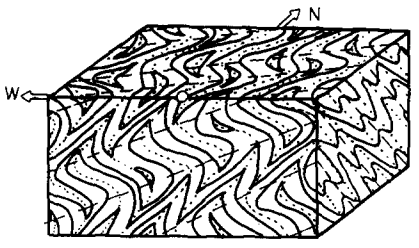


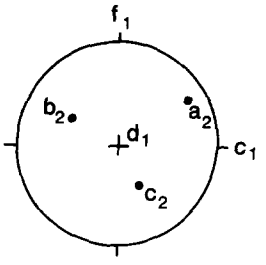


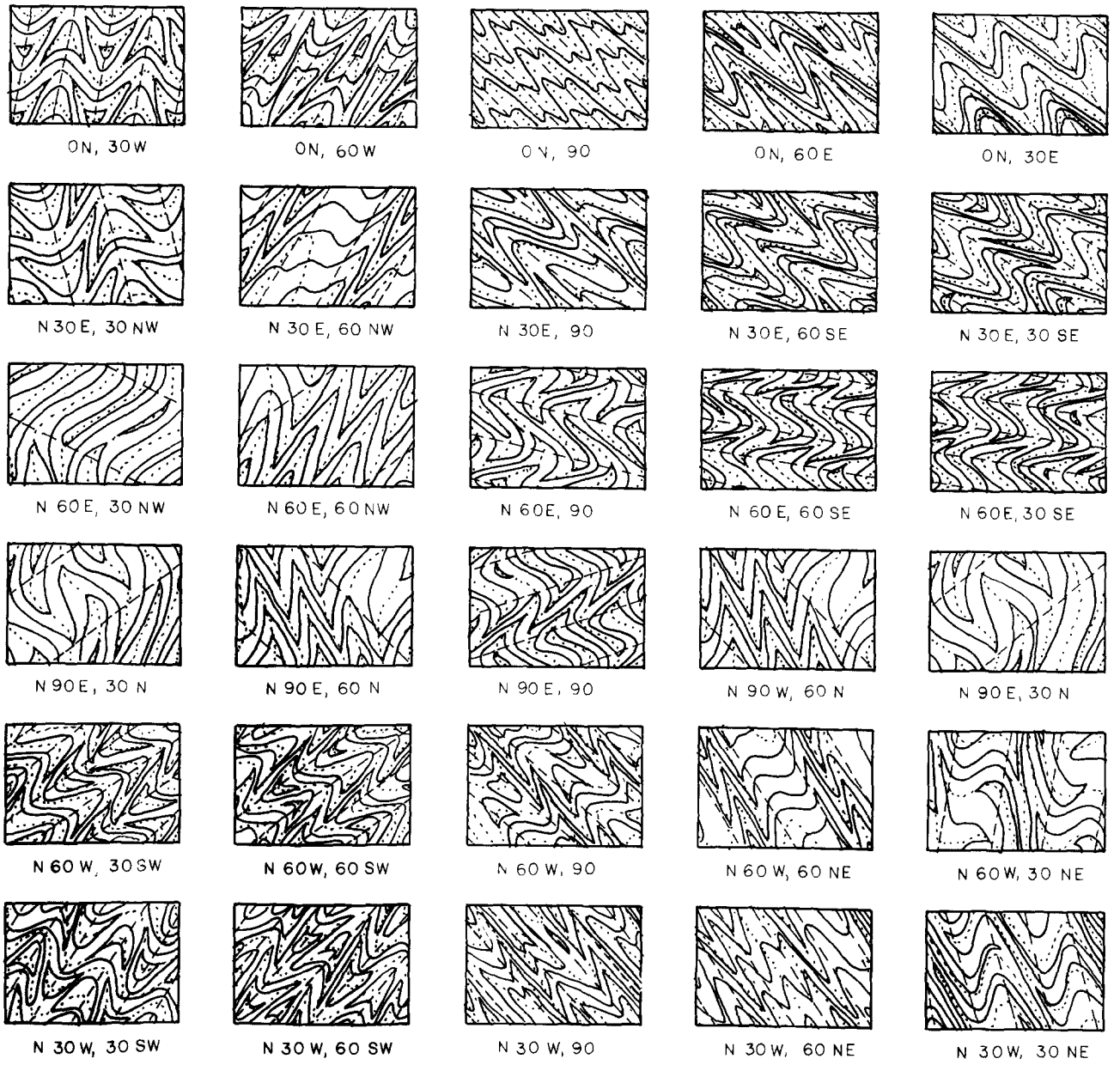


Fig. 8. This Figure and Fig. 9 show two type 2 refold structures that plot at the same point in the interior of Thiessen & Means' (1980) orientation volume. Conventions are as in Fig. 3, and with $\alpha = 68°$, $\beta = 45°$, $\gamma = 45°$, $\delta = 103°$.

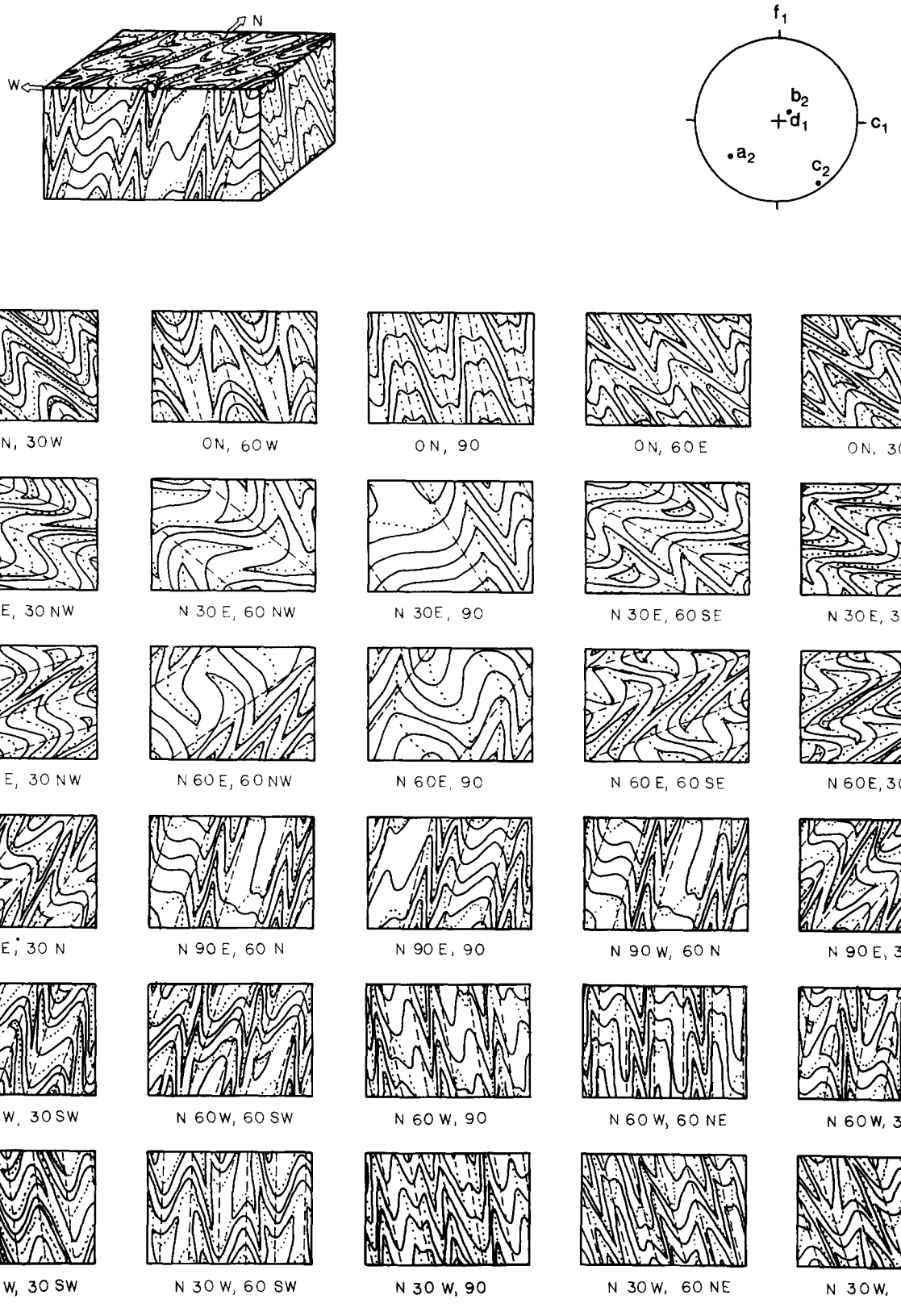


Fig. 9. See Fig. 8. $\alpha = 68°$, $\beta = 45°$, $\gamma = 45°$, $\delta = 133°$.

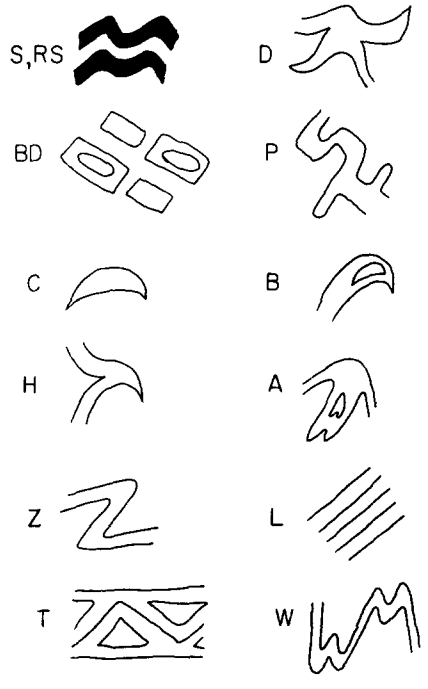


Fig. 10. The various two-dimensional interference patterns that have been identified in this and previous studies. See text for description.

Figure 11 shows the ranges of the different two-dimensional interference patterns, as projected onto the $\beta$–$\gamma$ plane. Sine waves (S) are not plotted because they were found to occur everywhere in types 0, 1 and 2. Repeated sine waves are also not included since their range has already been defined. Computer output for every 15°-combination of $\alpha$, $\beta$ and $\gamma$ was examined for the patterns shown in Fig. 10. When any of these patterns appeared at any $\beta$–$\gamma$ coordinate pair, it would appear at all the values checked. In other words, the ranges seem to be continuous as one moves vertically in the orientation volume (i.e. as $\alpha$ is varied). The only exception to this is the repeated sine wave pattern. Figure 11 was generated looking at nearly a thousand sections through refolds. Although this may seem like a considerable number, the boundaries shown on Fig. 11 are only approximate, and most are gradational.

## DISCUSSION AND CONCLUSIONS

Interpretation of refold patterns that occur on outcrops or maps is often a difficult task. The figures presented show that there are virtually an infinite number of possible two-dimensional interference patterns. These were all developed using very tight constraints of symmetric first folds and simple sinusoidal waves for the first and second waveforms. If these constraints are removed, then yet another level of variations of patterns becomes possible. However, the picture is not as bleak as these realizations might seem to make it. There are recognizable general groups of patterns which are summarized in Fig. 11. Type 1 refolds can be characterized by sine wave, basin and dome, and tear drop patterns. Type 2 refolds will create sine wave, repeated sine wave, dog's tooth, S and Z, M and W, crescent, hook, arrow, and bird's head patterns. Type 3 refolds might form hooks, straight lines, and occasional S and Z patterns. The triangular refolds (type 1 →2) are characterized by triangles, crescents, S's and Z's, dog's teeth, perpendiculars, sine waves and hooks.

This entire discussion assumes that bedding behaves passively, and that the folds are similar concentric folds. In the real world, few folds behave in this ideal manner, and so there is an additional reason for departure of actual refold geometry from the idealized patterns analyzed here. It is entirely possible that more competent layers or anisotropic elements within the rock will control the refolding, creating patterns not seen in this exercise.

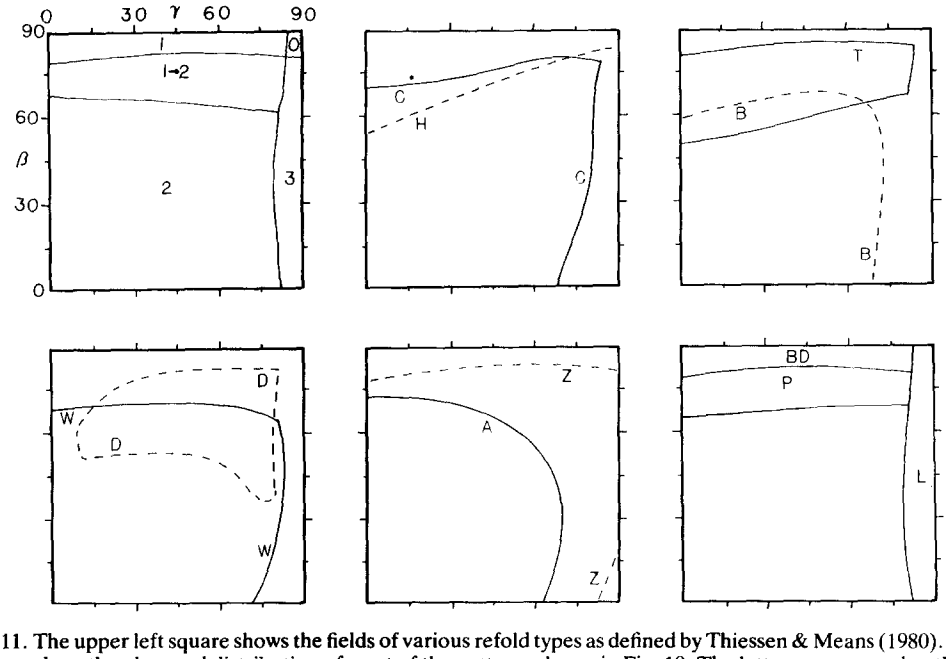


Fig. 11. The upper left square shows the fields of various refold types as defined by Thiessen & Means (1980). The remaining squares show the observed distribution of most of the patterns shown in Fig. 10. The letters correspond to those of Fig. 10. Boundaries are approximate and gradational.

Figure 1 demonstrates the difficulty in analyzing one single refold that might be seen on a map or outcrop. A single two-dimensional interference pattern can be created by an infinite variety of three-dimensional structures. Several types of data can be used to constrain the geometries involved, but to unravel totally the geometry of the refold is a more complex task. To completely characterize a refold, one must know, for both fold generations, the hinge directions, axial plane orientations, waveforms, amplitudes, and some measure of how close they are to ideal similar cylindrical folds, In addition, one needs the axis of second folding motion ($b_2$). Two techniques exist that will allow all these data to be acquired. Carey (1962, reviewed by Ragan 1973) devised an unfolding technique that works for type 3 (coaxial) refolds, but not for any other types. Thiessen & Haviland (1986) present a method for the analysis of type 1 and type 2 refolds. This latter technique will not work with coaxial refolds, so the two techniques are mutually complementary. Thiessen & Haviland's (1986) technique requires three-dimensional control on the geometry of the refold structure, and has been applied by them to a rock sample cut into serial sections.

Refolds become economically important when they occur in mining districts. Axial reef ore bodies, for example, are concentrated along hinge lines. The ore is thus intimately involved with the folding (Stauffer 1968), and exploration and development in such districts have to rely upon refold analysis. Thiessen & Brown (1985) discuss refolds in mining districts and demonstrate, for an example in the Galena–Roubaix district of South Dakota, the necessary modification of exploration techniques.

The analysis in this paper demonstrates the wide variety of possible refold patterns that could appear on a map or outcrop. Many of these patterns would probably not be readily recognized by most geologists as being caused by simple refolds, particularly if they saw only portions of the entire structure, as would be likely in most mapping projects. A glance at the figures accompanying this report will show yet another problem in the recognition of simple refold patterns. The interference pattern often appears much more complex than the refolding geometry that produced it. Figures 4 and 7 were both generated by simple sine waves interacting at right angles to each other. If one were mapping rocks that had undergone either of these refolding geometries, one could see an incredibly complex series of patterns on individual outcrops. In both figures, the tightness of folds changes drastically depending on the view. The kinematic axial planes (shown with dashes and dots) will not coincide with the observed local axial surface traces due to the variation in orientation of bedding (Ramsay 1967). Carey (1962) pointed out that the first folds are often tightened quite a bit as they are folded across the second folds. What started out as an open sine wave may end up tight or isoclinal.

For perfect type 0 and type 3 refolds, one would expect to see the exact same two-dimensional pattern on all parallel cross-sections. However, with the other types of refolds, one would expect to see the patterns evolve on successive sections. If, for example, one was slicing through a basin, one would see a circular or oval outcrop pattern reduce in size and finally disappear as one looked at deeper levels of the basin. The more complex refold patterns shown in Figs. 3, 4 and 6–9 would also evolve with sectioning, but in more complex fashions. However, examining many such cases reveals that the general appearance and patterns will not appreciably alter.

Appreciation of all the above complications only comes with experience with refolds and their complexities. This experience can only be gained by study of refold models, such as those presented herein, or of actual refolds in the field.

*Acknowledgements*—I would like to thank helpful discussions and critical reviews by W. Means, A. J. Watkinson, S. P. Brown, P. Hudleston and two anonymous reviewers. Part of this work was done while I held a National Science Foundation Doctoral Fellowship. I am also indebted to my wife, Daleah, for helping with the massive amounts of drafting involved in the diagrams of this report, and also for editing the text.

## REFERENCES

Brown, S. P. 1967. Anatomy of a refold—an empirical approach. *Empire State Geogram* **5**, 9–14.

Carey, S. W. 1962. Folding. *J. Alberta Soc. Petrol. Geol.* **10**, 95–144.

Holmes, A. & Reynolds, D. L. 1954. The superposition of Caledonian folds on older fold systems in the Dalradians of Malin Head, Co. Donegal. *Geol. Mag.* **91**, 417–444.

O'Driscoll, E. S. 1962. Experimental patterns in superimposed similar folding. *J. Alberta Soc. Petrol. Geol.* **10**, 145–167.

Ragan, D. M. 1973. *Structural Geology, an Introduction to Geometrical Techniques* (Second Edition). John Wiley, New York.

Ramsay, J. G. 1967. *Folding and Fracturing of Rocks*. McGraw-Hill, New York.

Stauffer, M. R. 1968. The tracing of hinge-line ore bodies in areas of repeated folding. *Can. J. Earth Sci.* **5**, 69–79.

Thiessen, R. L. & Brown, S. 1985. Computer simulation of a refolded mining district: Galena–Roubaix, S. D. *Abs. with Prog. geol. Soc. Am.* **17**, 267.

Thiessen, R. L. & Haviland, T. 1986. A technique for the analysis of refold structures. *J. Struct. Geol.* **8**, 191–200.

Thiessen, R. L. & Means, W. D. 1980. Classification of fold interference patterns: a re-examination. *J. Struct. Geol.* **2**, 311–316.

Watkinson, A. J. 1981. Patterns of fold interference: influence of early fold shapes. *J. Struct. Geol.* **3**, 19–23.